Singular perturbation analysis of the pore creation transient

John C. Neu[1,2] and Wanda Krassowska[2,*]
[1]*Department of Mathematics, University of California at Berkeley, Berkeley, California 94720, USA*
[2]*Department of Biomedical Engineering, Duke University, Durham, North Carolina 27708, USA*
(Received 19 February 2006; revised manuscript received 2 August 2006; published 27 September 2006)

Electroporation, in which electric pulses create transient pores in the cell membrane, is an important technique for drug and DNA delivery. Electroporation kinetics is mathematically described by an advection-diffusion boundary value problem. This study uses singular perturbation to derive a reduced description of the pore creation transient in the form of a single integrodifferential equation for the transmembrane voltage $V(t)$. The number of pores and the distribution of their radii are computed from $V(t)$. The analysis contains two nonstandard features: the use of the voltage deviation to peel away the strong exponential dependence of pore creation upon the transmembrane potential, and the autonomous approximation of the pore evolution. Comparing the predictions of the reduced equation with the simulations of the original problem demonstrates that this analysis allows one to predict with good accuracy the number and distribution of pores as a function of the electric pulse strength.

DOI: 10.1103/PhysRevE.74.031917 PACS number(s): 87.16.Ac, 87.16.Dg, 87.50.Rr

I. INTRODUCTION

Electroporation refers to the creation of water-filled pores in the lipid bilayer of the cell membrane under the influence of strong electric pulses. Electroporation can occur as a result of power-line accidents [1] but it also has beneficial applications in biotechnology and medicine: because the pores reseal in the matter of seconds to minutes, electroporation is used to deliver biologically active molecules, drugs or DNA, into cells [2–4]. While electroporation-mediated DNA delivery emerges as a potential technique for nonviral gene therapy, its effectiveness depends strongly and often unpredictably on experimental factors. Thus, a better understanding of the electroporation process, coming from mathematical modeling and analysis, would be very useful in facilitating progress in practical applications of this technique.

Experimental and theoretical studies of electroporation reveal that it consists of a sequence of phases. Briefly, electroporation starts with the application of an electric pulse that charges the cell membrane (charging phase). When the voltage difference across the membrane (i.e., transmembrane voltage V) is sufficiently large (0.5–1 V, depending on the cell type), pores are created (creation transient). Water-filled hydrophilic pores are created with a radius $r_* \approx 0.5$ nm but grow rapidly. The creation and growth of the pores decreases the resistance of the membrane, first slowing the increase and eventually decreasing the transmembrane voltage V. Once V drops below the threshold value, the creation ceases and a new phase starts, during which the existing pores expand in order to relieve the tension of the membrane. This pore evolution phase can lead to accumulation, in which a large number of pores assume the same radius, or to coarsening, in which one pore grows to a giant size and the remaining pores shrink and eventually reseal. For typical pulse strengths, the pore evolution phase lasts a few milliseconds. After the pulse is turned off, V drops to zero, causing the pores to shrink to a radius of approximately 1 nm, although post-shock coarsening is also possible. This shrinkage phase is very fast (microseconds) and it is followed by the resealing phase, during which the pores disappear and the integrity of the lipid bilayer is restored. Resealing takes seconds to minutes, depending on the cell type and experimental conditions.

Electroporation presents rather peculiar challenges to theoretical analysis, both by numerical simulations and by singular perturbation analysis. Theoretically, the process of electroporation is described by an advection-diffusion boundary value problem (BVP). Under conditions corresponding to most practical applications, the BVP is stiff because of strong exponential dependence of the pore creation rate upon the square of the transmembrane voltage: increments of V as small as 0.02 V can result in a threefold increase in the pore creation rate. Thus, initial studies of electroporation that involved direct numerical solution of this BVP required very small spatial and temporal discretization steps of 5 pm and 1 ps, respectively [5]. Consequently, these early studies could investigate electroporation process for only very short intervals, on the order of microseconds. While it was sufficient for applications of electroporation that involved ultrashort pulses, such as irreversible breakdown and rupture of the artificial lipid bilayers and biological cells [5,6], or reversible electroporation with a large number of small pores [7,8], other applications, such as gene delivery that require pulses on the order of milliseconds, were beyond the reach of these methods. Our previous research has asymptotically reduced the governing BVP to an ordinary differential equation (ODE) for pore creation [9] and a set of ODEs for the evolution of pore radii [10]. Using ODEs avoids the necessity of solving a BVP, and the time step needed for a convergent solution is 3–5 orders of magnitude larger. This advance opened a possibility of studying longer pulsing protocols associated with gene delivery [11].

Nevertheless, simulations of electroporation that are based on creating *individual* pores and tracking evolution of their radii are expensive. In particular, during an early part of

*Corresponding author. FAX: 919-684-4488; Electronic address: wanda.krassowska@duke.edu

the creation transient, the number of pores and their radii must be tracked very accurately, which requires small time steps. Any errors in the number and distribution of pore radii would propagate to the transmembrane voltage. As we have just seen, small errors in V would be greatly amplified, resulting in a large difference in the creation rate and, consequently, the number of pores would be predicted incorrectly. Singular perturbation analysis comes to mind as a standard medicine for stiff problems and the prospect that it can produce reduced equations that accurately approximate the results of expensive simulations is tempting. The core content of this paper is in fact a singular perturbation analysis whose reduced equations still require numerical evaluation, albeit much smaller and cheaper.

The limit process of this perturbation analysis is nonstandard. The first essential idea is to peel away the strong exponential dependence of pore creation rate upon the transmembrane voltage V. Typically, the membrane rapidly charges until the V reaches a threshold and then rapid pore creation prevents V from increasing much beyond that value. Thus, most of the creation happens within the narrow range of transmembrane voltage. The narrowness of this voltage range serves as the essential small parameter, ε, and its value is established by a standard scaling argument. Scaling units of time, pore radius, and pore density are determined from dominant balances applied to all the equations of the advection-diffusion BVP.

The next step is to formulate the nondimensional version of the advection-diffusion BVP, containing ε as a gauge parameter. The $\varepsilon \to 0$ asymptotic solution of the dimensionless BVP exploits a second nonstandard idea. It turns out that the evolution of pore radii during the creation transient is close to autonomous: Specifically, there is an adaptive time variable related to the physical time so that the growth rate of pore radii relative to this adaptive time can be approximated by a given function of radius, which has no explicit time dependence. Within this autonomous approximation, it is possible to reduce the full system of electroporation equations to a single integrodifferential equation for the transmembrane voltage, without further approximations. Once the transmembrane voltage is known, other observables, such as the pore density distribution and their effect on the membrane resistance readily follow.

The analysis presented here focuses on the pore creation transient. Section II is the mathematical formulation of electroporation kinetics in the form of an advection-diffusion boundary value problem. Section III determines the small parameter ε, and presents the dominant balance arguments that yield the scaling units of time, pore radius, and pore density. The nondimensional boundary value problem and its parameters are presented in Sec. IV. Section V presents the autonomous approximation, which reduces the full BVP to a single integrodifferential equation for the transmembrane voltage $V(t)$.

Section VI presents the derivation of this integrodifferential equation and the collateral determination of the pore number and the pore radii distribution associated with it. Finally, Sec. VIII compares the predictions of the asymptotic formulas developed here with brute-force numerical simulation of the pore creation process.

II. MATHEMATICAL FORMULATION OF THE KINETICS OF ELECTROPORATION

The evolution of pores is described by an advection-diffusion partial differential equation (PDE) [10],

$$\partial_t n + \partial_r\{Un - D\partial_r n\} = 0 \quad \text{in } r \geqslant r_*, \tag{1}$$

where the dependent variable is $n(r,t)$, the pore density distribution, such that at a given time t, the number of pores (per unit area) with radii between r and $r+dr$ is $n(r,t)dr$. The diffusion term, $\partial_r(D\partial_r n)$, describes random fluctuation of pore radii caused by thermal energy; the value of the diffusion coefficient D is given in Table I. The advection term, $\partial_r(Un)$, describes the changes in pore radii that are driven by minimization of the energy of the bilayer [10]. The advection velocity U is given by

$$U = \frac{D}{kT}\left[\frac{V^2 F}{1 + r_h/(r + r_t)} + 4\beta\left(\frac{r_*}{r}\right)^4 \frac{1}{r} - 2\pi\gamma + 2\pi\sigma r\right] \quad \text{in } r \geqslant r_*, \tag{2}$$

where the four terms correspond for the components of the bilayer energy as follows: the first term accounts for the electric energy induced by the transmembrane voltage V [12], the second, for the steric repulsion of lipid heads [9], the third, for the line tension acting on the pore perimeter [13], and the fourth, for the surface tension of the surrounding membrane [10]. The values of parameters F, r_h, r_t, β, and γ are given in Table I. In (2), σ is an effective surface tension of the membrane,

$$\sigma = \sigma_0 - 4\sigma' \int_{r_*}^{\infty} \pi r^2 n dr, \tag{3}$$

where the second term shows that the presence of pores decreases the initial membrane tension σ_0. Equations (1)–(3) can be considered as a nonlinear extension of the Smoluchowski equation introduced in the 1970s to describe the behavior of pores [3,7,13].

For the purpose of this study, we assume that pores are created with the initial radius r_* at a rate $\alpha e^{(V/V_{ep})^2}$ per unit area [9], where constants α and V_{ep} are given in Table I. In absence of resealing, which is not relevant during the creation transient, we have

$$\frac{d}{dt}\int_{r_*}^{\infty} n dr = \alpha e^{(V/V_{ep})^2}. \tag{4}$$

The theoretical basis for the exponential creation rate on the right-hand side of (4) is explained in Ref. [7]. There is no sharp threshold for pore creation: as expected from (4), any $V > 0$ will create pores but weak pulses may require very long time [14]. In practice, both in the model and in experiments, one sees an *apparently* sharp increase in pore formation as V increases through a narrow range about "threshold" voltage. In this model, the "threshold" voltage is well approximated by $4V_{ep} = 1.032$ V, where V_{ep} is the characteristic voltage of electroporation given in Table I.

TABLE I. Parameters of the electroporation model.[a]

Parameter	Value	Nondimensional value[b]	Scaling unit
α, creation rate coefficient	1×10^{9} m^{-2} s^{-1}		
V_{ep}, characteristic voltage of electroporation	0.258 V		
r_*, minimum radius of hydrophilic pores	0.5×10^{-9} m	0.03203	$[r]$
D, diffusion coefficient for pore radius	5×10^{-14} m^2 s^{-1}	3.679×10^{-4}	$[r]^2/[t]$
β, steric repulsion energy	1.4×10^{-19} J	0.01203	V_r^2F $[r]$
γ, edge energy	1.8×10^{-11} J m^{-1}	0.02415	V_r^2F
σ_0, tension of the bilayer without pores	1×10^{-3} J m^{-2}	0.02094	$V_r^2F/[r]$
σ', tension of hydrocarbon-water interface	2×10^{-2} J m^{-2}	0.4188	$V_r^2F/[r]$
F, max electric force for $V=1$ V	0.70×10^{-9} N V^{-2}		
r_h, characteristic length for electric force	0.97×10^{-9} m	0.06214	$[r]$
r_t, correction for toroidal pores	0.31×10^{-9} m	0.01986	$[r]$
C_m, surface capacitance of the membrane	10^{-2} F m^{-2}		
R_m, surface resistance of the membrane	0.5 Ω m^2		
A, total area of lipid bilayer[c]	1.26×10^{-9} m^2		
R_s, series resistance[d]	10^5 Ω		
τ, charging time constant[e]	1.26×10^{-6} s	0.7009	$[t]$
g, conductivity of the solution (Tyrode's)	2 S m^{-1}		
h, membrane thickness	5×10^{-9} m	0.3203	$[r]$
T, absolute temperature (37 °C)	310 K		

[a]Sources of all values are given in Ref. [11].
[b]Only for parameters appearing in reduced equations.
[c]Assuming spherical cell of a 10 μm radius.
[d]Chosen to give the charging time constant close to that of a cell.
[e]Computed as $R_sC=R_sC_mA$.

From (4) and (1), one can formulate a boundary condition (BC) at $r=r_*$,

$$\partial_r(Un - D\partial_r n)(r_*,t) = \alpha e^{(V/V_{ep})^2}. \tag{5}$$

The initial condition (IC) is $n(r,0)\equiv 0$, which means that a membrane has no pores before the electric pulse is applied.

To determine a unique solution for $n(r,t)$, the time evolution of the transmembrane voltage $V(t)$ must be given. V is a dynamical variable and its evolution depends on the experimental setup. This study assumes the simplest experimental setup: a uniformly polarized membrane, represented by the capacitance C, resistance R, and by the current I_p through electropores (Fig. 1). The circuit of Fig. 1 can be interpreted as an idealized representation of a depolarized (or hyperpolarized) "polar" region of a single cell exposed to an external field [15] and the control parameter V_0 can be interpreted as the maximum transmembrane voltage induced in a cell by the external electric field. Thus, the evolution equation for the transmembrane voltage V is

$$R_sC\partial_t V = V_0 - \left(1 + \frac{R_s}{R}\right)V - R_sI_p, \tag{6}$$

where the combined current I_p through all pores is given by

$$I_p = VA\int_{r_*}^{\infty}\frac{n}{R_p + R_i}dr = VAg\int_{r_*}^{\infty}\frac{2\pi r^2}{2h + \pi r}ndr. \tag{7}$$

This formula assumes that voltage drop V occurs across the sum of the pore resistance, $R_p=h/(\pi g r^2)$, and the input resistance, $R_i=1/(2gr)$ [16]; parameters g and h are given in Table I. The derivation of Eq. (6) ignores the rest potential, V_{rest}, of the cell. To account for V_{rest}, V_0 in (6) would have to be replaced by $V_0+(R_s/R)\,V_{\text{rest}}$. Typically, $V_{\text{rest}}=-0.08$ V, so $(R_s/R)V_{\text{rest}}=2\times10^{-5}$ V, i.e., negligible compared to V_0, which is on the order of 1 V. Consequently, (6) is used with the initial condition $V=0$, which also ignores the rest potential of the cell.

In summary, the dynamics of pore density distribution $n(r,t)$ is determined by the advection-diffusion PDE (1), the creation BC (5), and the voltage evolution equation (6). Further details and the rationale for this model of pore creation and evolution can be found in our previous presentations [9–12].

III. CHOICE OF SCALING UNITS

Under pulsing protocols of practical relevance, nearly all pores are created in a narrow range of the transmembrane voltage, somewhat above 1 V (for parameters in Table I). Thus, it is convenient to describe pore creation using a rela-

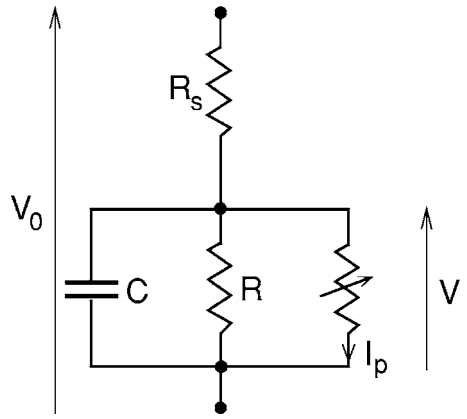

FIG. 1. Circuit representation of a uniformly polarized membrane of the surface area A. The capacitor $C=C_mA$ represents the total capacitance of the membrane and the constant resistor $R=R_m/A$ accounts for the flow of current through channel proteins (surface capacitance C_m and surface resistance R_m are given in Table I). The variable resistor accounts for the dynamically changing current through pores, I_p. The resistor R_s represents the series resistance of the experimental setup and V_0 is the external stimulus.

tive voltage deviation, $v \equiv (V-V_r)/V_r$, rather than its full value V. As a reference voltage V_r, we choose the "threshold" voltage, so that $V_r=4V_{ep}=1.032$ V. Using v and V_r, the creation exponential in (5) becomes

$$e^{(V/V_{ep})^2} = e^{(V_r/V_{ep})^2} \exp\left[\left(\frac{V_r}{V_{ep}}\right)^2 [(1+v)^2 - 1]\right].$$

Since $|v| \ll 1$, we approximate

$$e^{(V/V_{ep})^2} \approx e^{(V_r/V_{ep})^2} e^{2(V_r/V_{ep})^2 v}.$$

The above approximation motivates the choice of the scaling unit $[v]$ for deviation v,

$$[v] = \varepsilon \equiv \frac{1}{2}\left(\frac{V_{ep}}{V_r}\right)^2 = 0.03125, \tag{8}$$

as the value of v that increases the creation rate exponential by a factor of e. For $V_r=4V_{ep}$, $[v] \ll 1$, as assumed above. The scale $[v]$ also serves as a small parameter ε. Using (8), the voltage deviation is converted to its nondimensional form,

$$v = \frac{1}{\varepsilon}\frac{V-V_r}{V_r}. \tag{9}$$

The scaling units $[t]$, $[r]$, and $[n]$ of time, pore radius, and pore density, are determined by the *three dominant balances* that follow from the basic equations (1), (4), and (6). First, the advection velocity associated with the PDE (1) is U, defined in (2). The electrical component is expected to dominate in the pore creation transient, so the dominant balance associated with (1) is

$$\frac{[r]}{[t]} = \frac{DV_r^2 F}{kT}. \tag{10}$$

Second, the dominant balance associated with the creation identity (4) is

$$\frac{[n][r]}{[t]} = \alpha e^{(V_r/V_{ep})^2}. \tag{11}$$

Finally, we will develop the dominant balance associated with the voltage evolution equation (6). Recognizing that $R_s/R=2.4\times10^{-5}$ is small compared to one, we drop this term and, introducing the definition of I_p (7), we obtain

$$R_s C \partial_t V = V_0 - V - R_s V A g \int_{r_*}^{\infty} \frac{2\pi r^2}{2h+\pi r} n dr. \tag{12}$$

Here, V_0-V can be estimated from (8) as $2[v]=V_{ep}^2/V_r$, and the order of magnitude of the integral in (12) is $[r]^2[n]$. Hence, the dominant balance of terms on the right-hand side of (12) is

$$\frac{V_{ep}^2}{V_r} = R_s V_r A g [r]^2 [n] \quad \text{or} \quad \left(\frac{V_{ep}}{V_r}\right)^2 = R_s A g [r]^2 [n]. \tag{13}$$

From the three dominant balance equations (10), (11), and (13), we determine $[r]$, $[t]$, and $[n]$,

$$[r] = \sqrt{\frac{DV_{ep}^2 F}{kT\alpha R_s A g}} e^{-(1/2)(V_r/V_{ep})^2} = 1.56\times10^{-8} \text{ m}, \tag{14}$$

$$[t] = \frac{kT[r]}{DV_r^2 F} = 1.79\times10^{-6} \text{ s}, \tag{15}$$

$$[n] = \frac{\alpha[t]}{[r]} e^{(V_r/V_{ep})^2} = 1.02\times10^{18} \text{ m}^{-3}. \tag{16}$$

IV. NONDIMENSIONAL EQUATIONS AND PARAMETERS

The nondimensional equations contain nondimensional versions of the parameters. Their values, together with the scaling units, are given in columns 3 and 4 of Table I. The nondimensional effective tension σ is

$$\sigma = \sigma_0 - 4\sigma' \mu \int_{r_*}^{\infty} r^2 n dr, \tag{17}$$

where nondimensional parameter $\mu \equiv [r]^3[n]$ arises from scaling of the integral. The ratio $4\sigma'\mu/\sigma_0$ measures the decrease in tension due to pores relative to the tension of intact bilayer. Its value is 3.1×10^{-4}, indicating that during creation transient, the effect of the pores on the membrane tension is negligible.

The nondimensional version of the advection-diffusion PDE (1) is

$$\partial_t n + \partial_r (Un - D\partial_r n) = 0 \quad \text{in } r > r_*, \tag{18}$$

and the nondimensional version of the creation BC (5) is

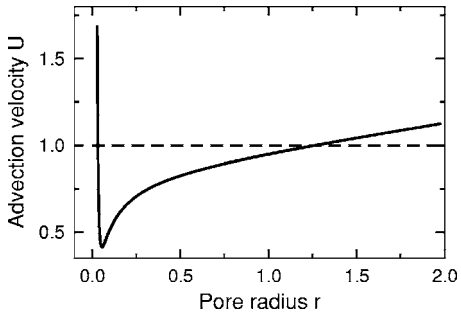

FIG. 2. Advection velocity as a function of the pore radius. The solid line shows the advection velocity computed from (23), assuming $\varepsilon=0$ and $\sigma=\sigma_0$; the dashed line is a constant-value approximation $U\equiv 1$. Both pore radius and advection velocity are nondimensional.

$$\partial_r(Un - D\partial_r n)(r_*,t) = e^{[(1+\varepsilon v)^2-1]/(2\varepsilon)}. \tag{19}$$

In the limit $\varepsilon\to 0$, the right-hand side of (19) asymptotes to the *ε-independent* limit e^v, which is the essential point of the unit $[v]$ in (8).

A preliminary form of the nondimensional voltage evolution equation (6) is

$$\tau\varepsilon\partial_t v = \varepsilon(v_0 - v) - R_s A g[r]^2[n](1+\varepsilon v)\int_{r_*}^{\infty}\frac{2\pi r^2}{2h+\pi r}ndr.$$

Here, v_0 is the nondimensional voltage deviation corresponding to V_0, computed from (9), and τ is the nondimensional charging time constant from Table I. By the third dominant balance (13), $R_s A g[r]^2[n]=2\varepsilon$ and there is a cancellation of ε, leaving

$$\tau\partial_t v = (v_0 - v) - 2(1+\varepsilon v)\int_{r_*}^{\infty}\frac{2\pi r^2}{2h+\pi r}ndr. \tag{20}$$

V. REDUCED DYNAMICS

The scaled values of many parameters in Table I are conspicuously small. The nondimensional diffusion coefficient D is the smallest, so henceforth we will neglect diffusion terms in the PDE (18) and BC (19). The diffusionless versions of (18) and (19) are

$$\partial_t n + \partial_r(Un) = 0 \quad \text{in } r > r_*, \tag{21}$$

$$(Un)(r_*,t) = e^{(v+\varepsilon v^2/2)(t)}, \tag{22}$$

where U is the nondimensional advection velocity,

$$U = \frac{(1+\varepsilon v)^2}{1+r_h/(r+r_t)} + 4\beta\left(\frac{r_*}{r}\right)^4\frac{1}{r} - 2\pi\gamma + 2\pi\sigma r. \tag{23}$$

Equations (21) and (22) subject to the IC $n(r,0)\equiv 0$ in $r \geqslant r_*$ is an *advection signaling problem*.

This advection velocity can be further reduced. Considering the smallness of parameters r_h, r_t, β, γ, and σ, (column 3 of Table I) one might expect U to be close to the uniform value of 1. However, Fig. 2 demonstrates that such an approximation is not acceptable. Instead, the asymptotic reduction of U will be based on an autonomous approximation. Note that the explicit time dependence of U comes from only two sources: the integral term in the effective tension σ (17) and the factor $(1+\varepsilon v)^2$ in the electrical component of U. The former is expected to be a weak effect, due to the smallness of the ratio $4\sigma'\mu/\sigma_0$, and the time dependent σ can be replaced by the constant σ_0. The latter can be absorbed by renormalization of time. Introduce in place of time t the adaptive time ξ so that

$$\frac{d\xi}{dt} = (1+\varepsilon v)^2.$$

Regarding $v=v(\xi)$ as a function of ξ, the relation between t and ξ is

$$t = \int_0^{\xi}\frac{d\xi'}{[1+\varepsilon v(\xi')]^2}. \tag{24}$$

With the adaptive time, problem (21) and (22) is converted into a signaling problem for $n(r,\xi)$,

$$\partial_\xi n + \partial_r\left(\frac{U}{(1+\varepsilon v)^2}n\right) = 0 \quad \text{in } r > r_*, \tag{25}$$

$$\left(\frac{U}{(1+\varepsilon v)^2}n\right)(r_*,\xi) = \left(\frac{e^{v+\varepsilon v^2/2}}{(1+\varepsilon v)^2}\right)(\xi). \tag{26}$$

The renormalized advection velocity appearing in (25) and (26) is

$$\frac{U}{(1+\varepsilon v)^2} = \frac{1}{1+r_h/(r+r_t)} + \frac{1}{(1+\varepsilon V)^2}\left[4\beta\left(\frac{r_*}{r}\right)^4\frac{1}{r} - 2\pi\gamma + 2\pi\sigma_0 r\right]. \tag{27}$$

The first term on the right-hand side is the dominant electric component, independent of ξ. Explicit ξ dependence is confined to the remaining steric, line, and area components. They are already small compared to the electric component, so the effect of the explicit ξ dependence in εv is reduced. Hence, the renormalized advection velocity (27) is replaced by the autonomous approximation U^0,

$$U^0 = \frac{1}{1+r_h/(r+r_t)} + 4\beta\left(\frac{r_*}{r}\right)^4\frac{1}{r} - 2\pi\gamma + 2\pi\sigma_0 r. \tag{28}$$

VI. INTEGRODIFFERENTIAL INITIAL VALUE PROBLEM FOR VOLTAGE DEVIATION

In this section we shall show that with the autonomous approximation (28) of the advection velocity, the full problem for $n(r,t)$ and $v(r)$ reduces to a single integrodifferential initial value problem (IVP) for $v(\xi)$. First, multiply the PDE (25) by U^0 to obtain

$$\partial_\xi(U^0 n) + U^0\partial_r(U^0 n) = 0. \tag{29}$$

Note that multiplication by U^0 commutes with ∂_ξ because $U^0=U^0(r)$ is independent of ξ. It follows from (29) that $U^0 n$

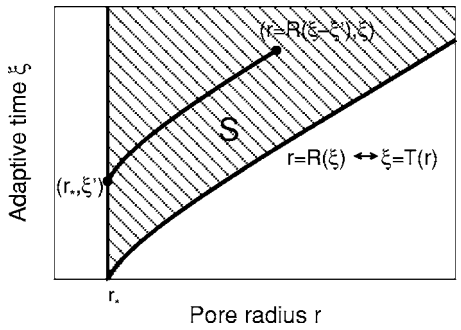

FIG. 3. Support S of the pore density distribution $n(r,\xi)$. Left boundary is the vertical line corresponding to r_*, the smallest radius of all pores. Bottom-right boundary is the trajectory $R(\xi)$ of the first pore, created at $\xi=0$. A pore created at time ξ' has at the later time ξ radius $r=R(\xi-\xi')$.

is constant along integral curves of the ODE,

$$\frac{dr}{d\xi} = U^0(r). \tag{30}$$

Denote the solution of (30) with $r(0)=r_*$ by $r=R(\xi)$. $R(\xi)$ is the evolution of the first pore radius in renormalized time ξ. More generally, the solution of (30) with $r(\xi')=r_*$ is $r=R(\xi-\xi')$ for $\xi \geqslant \xi'$.

Since $U^0 n$ is constant along $r=R(\xi-\xi')$, $(U^0 n)[R(\xi-\xi'),\xi]=(U^0 n)(r_*,\xi')$. Thus, the BC (26) with $U/(1+\varepsilon v)^2$ replaced by U^0 implies

$$(U^0 n)[R(\xi-\xi'),\xi] = \left(\frac{e^{v+\varepsilon v^2/2}}{(1+\varepsilon v)^2}\right)(\xi'). \tag{31}$$

Equation (31) determines $n(r,\xi)$ on its support S: $\xi>0$, $0<r<R(\xi)$. The procedure is illustrated in Fig. 3. Take (r,ξ) in S; determine ξ' as a function of (r,ξ) by inverting $r=R(\xi-\xi')$ to obtain $T(r)=\xi-\xi'$ so that $\xi'=\xi-T(r)$. Using $T(r)$, (31) determines $n(r,\xi)$ as

$$n(r,\xi) = \frac{1}{U^0(r)}\left(\frac{e^{v+\varepsilon v^2/2}}{(1+\varepsilon v)^2}\right)(\xi - T(r)). \tag{32}$$

Now we turn to the voltage evolution equation (20). Using the renormalized time ξ and $n(r,\xi)$ from (32), we obtain

$$\tau(1+\varepsilon v)^2\frac{dv}{d\xi} = v_0 - v - 2(1+\varepsilon v)\int_{r_*}^{R(\xi)} \frac{2\pi r^2}{2h+\pi r} \times\left(\frac{e^{v+\varepsilon v^2/2}}{(1+\varepsilon v)^2}\right)(\xi - T(r))\frac{dr}{U^0(r)}. \tag{33}$$

We change the variable of integration from r to $\xi'=\xi-T(r)$. We have $r=R(\xi-\xi')$, so that $r=R(\xi)$ implies $\xi'=0$, and $r=r_*$ implies $\xi'=\xi$. Furthermore, since $r=R(\xi-\xi')$,

$$dr = \frac{dR}{d\xi}(\xi-\xi')(-d\xi') = -\frac{dR}{d\xi}(T(r))d\xi' = -U^0(r)d\xi'.$$

Hence, the transformed version of (33),

$$\tau(1+\varepsilon v)^2\frac{dv}{d\xi} = v_0 - v - 2(1+\varepsilon v)\int_0^{\xi} \frac{2\pi R^2(\xi-\xi')}{2h+\pi R(\xi-\xi')} \times\left(\frac{e^{v+\varepsilon v^2/2}}{(1+\varepsilon v)^2}\right)(\xi')d\xi', \tag{34}$$

constitutes the *integrodifferential equation* for $v(\xi)$.

Given the solution for $v(\xi)$, the pore density distribution follows from (32). The total pore density $N(\xi) \equiv \int_{r_*}^{\infty} n(r,\xi)dr$ has ξ-rate of change,

$$\frac{dN}{d\xi} = \int_{r_*}^{\infty} \partial_\xi n d\xi = -\int_{r_*}^{\infty} \partial_r\left(\frac{U}{(1+\varepsilon v)^2}n\right)dr = \left(\frac{e^{v+\varepsilon v^2/2}}{(1+\varepsilon v)^2}\right)(\xi),$$

as follows from (25) and (26). Hence, we obtain

$$N(\xi) = \int_0^{\xi} \frac{e^{v+\varepsilon v^2/2}}{(1+\varepsilon v)^2}d\xi. \tag{35}$$

The relation (24) between t and ξ can be used to convert v, n, and N from functions of ξ to functions of t.

VII. IGNITING ELECTROPORATION AND AN EFFECTIVE INITIAL CONDITION ON THE VOLTAGE

The initial value of the voltage is $V(0)=0$, and this corresponds to a large, negative value of the dimensionless voltage deviation $v(0)=-1/\varepsilon$. This value cannot be used as an IC for (34): the coefficient of the derivative on the left-hand side would become zero. It reflects the breakdown of the relation (24) between t and ξ when one tries to impose $v(0)=-1/\varepsilon$. An alternative, effective IC is derived.

First, we recognize that as long as the deviation $v(t)$ remains large and negative, the rate of pore creation, proportional to $e^{(v+\varepsilon v^2/2)}$, is exponentially small, and the current I_p is negligible. In this case, the solution for $V(t)$ reflects pure RC charging,

$$V(t) = V_0(1-e^{-t/\tau}). \tag{36}$$

In terms of the nondimensional voltage deviation v, (36) reads

$$v(t) = v_0 - \frac{1}{\varepsilon}(1+\varepsilon v_0)e^{-t/\tau} \tag{37}$$

in which all parameters are nondimensional (column 3 of Table I).

If the pulse strength V_0 is significantly less than the reference voltage V_r, then RC charging goes to completion with V approaching V_0, and the deviation v remains large and negative. For these V_0, no significant pore creation is expected to occur.

If V_0 is close to or above V_r, the pure RC charging breaks down when V approaches V_r, signaling the ignition of significant pore creation. The time t_1 and voltage v_1 of ignition is estimated by requiring that at times $t<t_1$, the pore density $N(t)$ should amount to less than one pore (hence subscript 1). The calculation of t_1 and v_1 proceeds as follows: From (21) and (22), nondimensional pore density $N(t)$ increases at the rate

$$\partial_t N = e^{v(t)+\varepsilon v^2(t)/2}. \tag{38}$$

Taking the limit $\varepsilon \to 0$, substituting into (38) the Taylor's expansion of the preignition approximation (37) for $v(t)$, and integrating from $t=0$ to t_1, one finds an estimate of $N(t_1)$,

$$N(t_1) = \frac{\tau}{v_0 - v_1} e^{v_1}.$$

This nondimensional pore density is converted into the expected pore number by multiplying by $[n][r]A$. Hence, the condition that the expected number of pores be no more than one at time t_1 is

$$[n][r]A \frac{\tau}{v_0 - v_1} e^{v_1} \leqslant 1. \tag{39}$$

In simulations, we compute v_1 from (39) and determine t_1 from (37) as

$$t_1 = \tau \ln \frac{1 + \varepsilon v_0}{\varepsilon (v_0 - v_1)}. \tag{40}$$

For $t > t_1$, the voltage deviation v is computed as the solution of the integrodifferential equation (34) subject to IC $v(\xi=0)=v_1$ and converting $v(\xi)$ to $v(t)$ using

$$t - t_1 = \int_0^{\xi} \frac{d\xi'}{[1 + \varepsilon v(\xi')]^2}. \tag{41}$$

VIII. COMPARISON OF THE SOLUTIONS TO THE REDUCED AND ORIGINAL PROBLEMS

The solution to the reduced problem was computed numerically by integrating Eq. (34) for $v(t)$ and Eq. (30) for $R(t)$ using Euler method. Simultaneously, integrals (35) for N and (24) for t were evaluated using the rectangular rule. The initial condition for voltage, v_1, was determined by finding the root of (39) using Newton's method; the initial time t_1 was computed from (40). At a prescribed time t, the pore density distribution $n(r,t)$ was computed from (32). The time step was 1 ns. All calculations were performed in nondimensional variables and the final results were converted into dimensional variables.

The solution to the original problem was computed as described in our previous presentations [10,11]. Briefly, the PDE (1) for $n(r,t)$ was reduced to a first order advection PDE by eliminating the diffusion term, and the method of characteristics was used to derive ODEs for the evolution of individual pore radii. The resulting set of ODEs, as well as equations for voltage V and pore density N were solved numerically using a midpoint method. By launching individual pores as they were created, the program attempted to reproduce *in silico* the electroporation process occurring in a membrane. At a prescribed time t, the pore density distribution was determined by dividing the range of pore radii into 50 bins and counting the number of pores in each bin. The same time step of 1 ns was used for all calculations.

Figure 4 shows the results of the original and the reduced problems for the pulse strength of 1.5 V. Panels (a)–(c) show

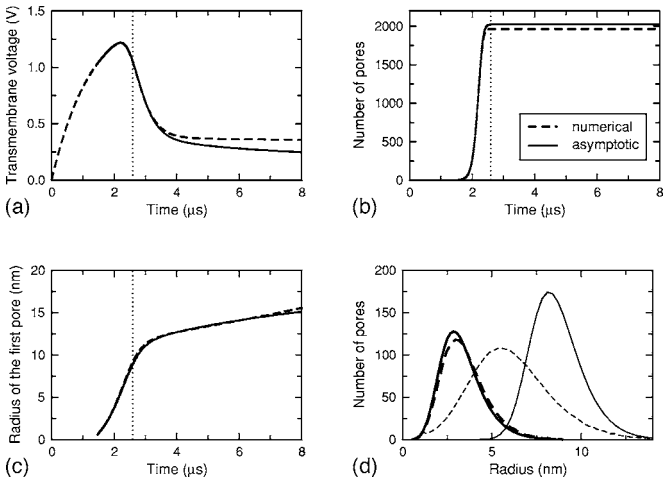

FIG. 4. Comparison of results obtained from the original problem (dashed lines) and from the asymptotic approximation (solid lines). (a) Transmembrane voltage, (b) number of pores, and (c) radius of the first pore are shown as functions of time. Vertical lines in panels (a)–(c) indicate the end of the creation transient, $t = 2.6$ μs, when the relative increase in pore density N per time step drops below 10^{-6}. (d) Distributions of pore radii are shown at the end of creation transient (thick lines) and at $t=8$ μs (thin lines). Pulse strength $V_0 = 1.5$ V.

that the voltage, the number of pores, and the radius of the first pore are computed very accurately during the creation transient and even a little beyond. Likewise, the distribution of pore radii is captured with good accuracy [panel (d), thick lines]. At later times, the solution to the reduced problem deteriorates. The most affected is the distribution of pore radii: because the tension coupling of pores was eliminated in the reduced problem (i.e., σ was replaced by σ_0), the reduced equations predict larger pores (maximum at 8.1 nm) than the original equations (maximum at 5.5 nm). Larger pores imply larger membrane conductance, which leads to a smaller voltage in panel (a).

Figure 5 shows the reference voltage V_r, evaluated from (14), in relation to voltages occurring during creation transient. V_1, at which pore creation begins, V_{peak}, the maximum

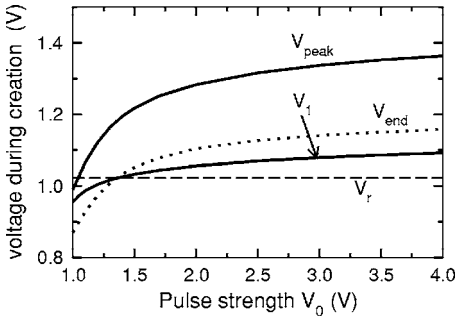

FIG. 5. Characteristic values of voltage during pore creation transient as a function of the pulse strength V_0. The dashed horizontal line is the reference voltage V_r evaluated from (14); V_1 is the dimensional value of voltage at which pore creation begins; V_{peak} is the maximum voltage during creation transient; and V_{end} (dotted line) is the voltage at which creation ends.

TABLE II. Differences[a] between solutions of the reduced and original problems. Labels: V_0, pulse strength in V. End, time of the end of creation transient in μs (also duration of the simulation). CC, correlation coefficient. RMSE, root mean square error relative to root mean square value. Speed, execution time of the reduced problem relative to the original problem.

		Relative difference in			Pore distribution		
V_0	End	Voltage	Pore number	First radius	CC	RMSE	Speed
1.0	12.4	0.00246	0.0686	0.0108	[b]	[b]	30.3
1.2	4.83	0.00241	0.0341	0.0024	0.9868	0.1033	3.64
1.5	2.60	0.00762	0.0300	0.0310	0.9954	0.0979	0.342
1.7	2.02	0.00909	0.0134	0.0419	0.9961	0.0902	0.149
2.0	1.53	0.00849	0.0135	0.0502	0.9979	0.0650	0.0398
2.5	1.10	0.00857	0.0478	0.0570	0.9981	0.0579	0.0148
3.0	0.86	0.00654	0.0708	0.0546	0.9934	0.1023	0.00850
3.5	0.71	0.00634	0.0872	0.0509	0.9844	0.1547	0.00481
4.0	0.61	0.00893	0.0999	0.0503	0.9766	0.1894	0.00209

[a]Calculated at the end of the creation transient, shown in the second column.
[b]Too few pores to meaningfully compare distributions.

voltage during creation transient, and V_{end}, at which creation ends, all increase with the pulse strength but remain in close proximity of V_r. Thus, as assumed in Sec. III, pores are created in a narrow range of voltages near V_r and voltage deviation v is indeed small compared to V_r.

Table II lists differences between the two solutions for pulse strengths $V_0=1-4$ V. $V_0=1$ V is the lowest value at which electroporation is observed in the model; $V_0=4$ V corresponds to a polarization of a 10 μm spherical cell by an electric field of 2.7 kV/cm, which exceeds typical fields used in drug and DNA delivery [4]. Simulations were run until the end of the creation transient (column 2), i.e., until the relative increase in pore density N per time step dropped below 10^{-6}. The table shows that the integrodifferential equation predicts $v(t)$ with remarkable accuracy: the relative difference between the two solutions is below 1%. The predictions of the number of pores and of the pore radii are less accurate but the difference between the solutions is confined to a few percent. The distribution of pores is the most sensitive to the approximations, especially at higher pulse strengths. Large root mean square error usually results from a slight shift of the two distributions in radius r, as seen in Fig. 4(d) (thick lines). The shape of the distribution is reproduced quite well, as indicated by the large values of the correlation coefficient.

IX. DISCUSSION

This study uses singular perturbation to reduce an advection-diffusion boundary value problem, traditionally used to describe electroporation, to a single integrodifferential equation for the transmembrane voltage $V(t)$. Once $V(t)$ is known, the number of pores and the distribution of their radii are computed by evaluating simple integrals. The analysis contains two nonstandard features: the use of the voltage deviation to peel away the strong exponential dependence of pore creation upon the transmembrane potential, and the autonomous approximation of the pore evolution.

The replacement of the renormalized advection velocity (27) by the autonomous approximation (28) is the only approximation made in deriving the integrodifferential equation (34) for v. If the steric, line, and surface terms are absent (i.e., parameters β, γ, and σ are set to zero) then there is no approximation and (34) is exact. In this sense, we are perturbing about the solution for purely electric force. The rationale is that during the pore creation transient, the electrical force is dominant, typically by a factor of 5–10.

The autonomous approximation used here is not the process $\varepsilon \to 0$: several occurrences of the small parameter ε remain in (34). In the $\varepsilon \to 0$ limit, the renormalized time ξ becomes identical to t, and the integrodifferential equation (34) becomes

$$\tau \frac{dv}{dt} = v_0 - v - 2\int_0^t \frac{2\pi R^2(t-t')}{2h + \pi R(t-t')} e^{v(t')} dt'. \qquad (42)$$

This only superficially simplifies (34) as it still requires computing the solution numerically and the additional terms in (34) do not really make the computations harder. Hence, in practice the limit equation (42) has no real simplicity advantage over (34). However, it has a noticeable effect on the accuracy. For a pulse strength $V_0=1.5$ V, Eq. (42) predicts 28.4% more pores with the first pore that is 10% smaller.

Even though the reduced problem determines only the creation transient, its ability to predict with good accuracy the number and distribution of pores for a given pulse strength can be applied in practice. In typical brute-force numerical simulations of electroporation, a disproportionate time is spent on the creation transient because a very small initial time step is needed to resolve rapid changes in V and N. Once the pores are created and N levels off, the time step can be increased and thus the pore evolution phase is computationally less demanding.

The reduced method has potential for speeding up the calculations. First, the RC charging phase, during which the

time step must be small to resolve V, can be bypassed altogether: the analysis allows one to estimate time t_1 when the creation of pores starts, and supplies the analytical solution for the preignition $V(t)$. The creation transient can also be computed more efficiently using the reduced method. As seen in the last column of Table II, the time savings are especially visible at higher pulse strengths, when a large number of pores are created and they must be followed individually in the original method. At low strengths, when very few pores are created but creation transients are long, the reduced method takes longer time. For example, the 1 V pulse requires 12.4 μs to create 14 pores. In this case, the reduced method is considerably slower because of the need to compute the convolution integral in (34). The time saving starts at $V_0=1.4$, when the pores number is in the thousands.

In comparing the computation speeds, note that no attempt was made to optimize the programs. In particular, the convolution integral in (34) can be computed using one of the fast algorithms [17], resulting in even larger time savings.

This paper concentrates on presenting a method of simulating the creation transient, which is the first phase of the electroporation process. To generate results that can be meaningfully compared to experiments, the model presented here can be combined with the model of later phases of electroporation (e.g., Ref. [10]). Such a combination would offer both substantial time savings and increase the accuracy of predicting the number of pores created by the pulse. As discussed in the Introduction, the accurate computation of the number of pores is difficult to obtain by purely numerical methods, yet it is a prerequisite for accurate evaluation of the pore distribution and transport through pores that is done in simulating later phases of electroporation. Thus, the method developed here may provide ground work for models that are capable of both qualitative and quantitative agreement with experiments and are efficient enough to investigate such problems of practical importance, like the dependence of drug and DNA uptake on pulsing parameters, temperature, and composition of the buffer solution.

ACKNOWLEDGMENT

This paper was supported in part by the National Science Foundation Grants Nos. BES-0401757 and DMS-0515616.

[1] R. C. Lee, D. J. Canaday, and S. M. Hammer, J. Burn Care Rehabil. **14**, 528 (1993).
[2] H. Potter, Anal. Biochem. **174**, 361 (1988).
[3] J. C. Weaver and Y. A. Chizmadzhev, Bioelectrochem. Bioenerg. **41**, 135 (1996).
[4] S. B. Dev, D. P. Rabussay, G. Widera, and G. A. Hofmann, IEEE Trans. Plasma Sci. **28**, 206 (2000).
[5] R. P. Joshi and K. H. Schoenbach, Phys. Rev. E **62**, 1025 (2000).
[6] I. G. Abidor, V. B. Arakelyan, L. V. Chernomordik, Y. A. Chizmadzhev, V. F. Pastushenko, and M. R. Tarasevich, Bioelectrochem. Bioenerg. **6**, 37 (1979).
[7] A. Barnett and J. C. Weaver, Bioelectrochem. Bioenerg. **25**, 163 (1991).
[8] S. A. Freeman, M. A. Wang, and J. C. Weaver, Biophys. J. **67**, 42 (1994).
[9] J. C. Neu and W. Krassowska, Phys. Rev. E **59**, 3471 (1999).
[10] J. C. Neu and W. Krassowska, Phys. Rev. E **67**, 021915 (2003).
[11] K. C. Smith, J. C. Neu, and W. Krassowska, Biophys. J. **86**, 2813 (2004).
[12] J. C. Neu, K. C. Smith, and W. Krassowska, Bioelectrochem. Bioenerg. **60**, 107 (2003).
[13] V. F. Pastushenko, Y. A. Chizmadzhev, and V. B. Arakelyan, Bioelectrochem. Bioenerg. **6**, 53 (1979).
[14] K. C. Melikov, V. A. Frolov, A. Ahcherbakov, A. V. Samsonov, and Y. A. Chizmadzhev, Biophys. J. **80**, 1829 (2001).
[15] T. R. Gowrishankar and J. C. Weaver, Proc. Natl. Acad. Sci. U.S.A. **100**, 3203 (2003).
[16] J. Newman, J. Electrochem. Soc. **113**, 501 (1966).
[17] R. Tolimieri, M. An, and C. Lu, *Algorithms for Discrete Fourier Transform and Convolution* (Springer-Verlag, New York, 1989).